Int. J. Nanosci. Nanotechnol., Vol. 12, No. 2, June 2016, pp. 71-77

Room Temperature Hydrogen Sensor Based on Single-Electron Tunneling Between Palladium Nanoparticles

Hadi Abbasi*, Hasan Sedghi and Mahdi Khaje

Department of Physics, Faculty of Science, University of Urmia, Urmia, Iran

(*) Corresponding author: h.abbasi@urmia.ac.ir
(Received: 06 March 2015 and Accepted: 11 July 2015)

Abstract

In this paper, we present the results of single-electron tunneling in two-dimensional (2D) hexagonal closed packed arrays of palladium nanoparticles. After inspecting the emergence of Coulomb blockade phenomena, we demonstrate the possibilities of using these arrays as a single-electron tunneling based hydrogen sensor. We assumed arrays of palladium nanoparticles with diameters of 3.5 and 6 nm based on the arrays synthesized experimentally. Using SIMON simulator, we obtained IV characteristics of equivalent circuits, consisting palladium nano-islands and tunneling junctions between source-drain electrodes, before and after exposing to hydrogen gas at room temperature. Resistance and capacitance of tunneling junctions were calculated according to the lattice parameter expansion of palladium nanoparticles at different pressures of hydrogen gas. We observed the change in the total resistance of the device before and after exposure to hydrogen. The obtained results indicate that this configuration show single-electron tunneling and can be used as the hydrogen gas sensor. This sensor can detect concentrations as low as 1.3% in air which is less than ammability concentration.

Keywords: *Monodisperse palladium nanoparticles, Hydrogen gas sensor, Single electron tunneling, Room temperature.*

1. INRODUCTION

Hydrogen gas due to its advantages such as cleanliness, natural abundance, and chemical reactivity has attracted a great deal of attention in industrial and engineering processes [1]. Nonetheless, concentrations of hydrogen gas more than 4% in air are highly flammable [2]. For this reason fast and reliable detection of hydrogen gas is required. Numerous hydrogen gas sensors have been developed and studied over the years [3]. These sensors operate based on the change in different properties of selective material upon adsorption and desorption of hydrogen. Palladium's specific size-dependent behavior upon adsorption and desorption of hydrogen gas makes palladium nanoparticles of interest for hydrogen gas sensing [4, 5].

By developing patterns of palladium nanoparticles, their specific behavior can be applied in order to detect hydrogen gas. Sang-Wook Kim and coworkers have synthesized monodisperse palladium nanoparticles with particle diameters of 3.5, 5, and 7 nm from the thermal decomposition of a palladium- surfactant complex. Their results show that, perfectly ordered arrays of close to identical nanoparticles (NPs) with hexagonal closed packed structure can be synthesized [6]. It must be noted that, this method results in synthesizing palladium nanoparticles with controlled size and spacing between them. An important fact about 2D hexagonal closed packed arrays is that, ultra large arrays of palladium nanoparticles can be produced. Jongnam Park and coworkers have succeeded to synthesize ultra large arrays of palladium nanoparticles up to 40 gr metal nanoparticles [7].

If the widths of the gaps between adjacent palladium nanoparticles are small, each less than 10 nm, then an applied voltage difference across the islands can transfer electrons on to, and off the islands by quantum mechanical tunneling [8]. The gaps then form tunnel barriers with an associated energy barrier. In such a systems single-electron tunneling occurs. Synthesized palladium nanoparticles will create multi-island single-electron arrays with tunneling barriers. The multi-island single-electron arrays of tunneling junctions are promising for the development of variety of devices due to their ultra-low power consumption, and high-sensitivity [9-12]. Their main advantages are higher threshold voltage of Coulomb blockade, less sensitivity to unwanted effects such as defects and background charges, higher operation temperature and ease of fabrication.

In this paper, we describe firstly single-electron tunneling in 2D hexagonal closed packed arrays of palladium nanoparticles based on the arrays synthesized by Sang-Wook Kim and coworkers [6]. We obtain size distribution and tunneling gaps of palladium nanoparticles from synthesized arrays. We assume the arrays with obtained specifications between source-drain electrodes and investigate the IV characteristics at room temperature. Then, we inspect possibilities of using these arrays as a single-electron tunneling based hydrogen sensor. The models and procedures used are provided in the following sections.

2. ASSUMPTION OF THE MODEL

We extracted size distribution and distance between nanoparticles from synthesized arrays. Gaussian distribution with narrow full widths at half maximum (FWHMs) were obtained for diameter of nanoparticles [6, 13]. The Gaussian Fit also confirmed the Gaussian distribution of size of nanoparticles. Also, Gaussian distribution was obtained for the distance between adjacent palladium nanoparticles. The extracted data from experimental results are shown in table 1.

Table 1. *A summary of parameters used in simulations (Extracted from experimental results [6,13]).*

Mean diameter of nanoparticles	3.5 nm	6 nm
Full width at half maximum	0.29 nm	0.7 nm
Lattice constant without hydrogen	3.908 A°	3.9 A°
Lattice constant at hydrogen pressure of 20 torr	3.96 A°	3.98 A°
Average tunneling gap width	1.9 nm	2.5 nm
FWHM for tunneling gap	0.35 nm	0.8 nm

We assumed several 2D hexagonal closed packed arrays of palladium nanoparticles with selected diameters of 3.5 and 6 nm for nanoparticles. Schematic diagram of the considered configurations are shown in Fig. 1. The arrays were biased by a source-drain voltage V_{ds} which was set from 0 to 4V. Fig. 2 shows equivalent circuits for assumed configuration of palladium nanoparticles in Fig. 1. Using SIMON 2.0 single-electron device simulator, we investigated I_{ds}-V_{ds} characteristics of equivalent circuits consisting palladium nano-islands and tunneling junctions. The results from simulations of 11×11 arrays are provided in results and discussion section. The SIMON 2.0 is a single-electron device and circuit simulator which employs Orthodox theory and Monte-Carlo methods in order to simulate the propagation of electrons in a wide variety of single-electron circuits [14].

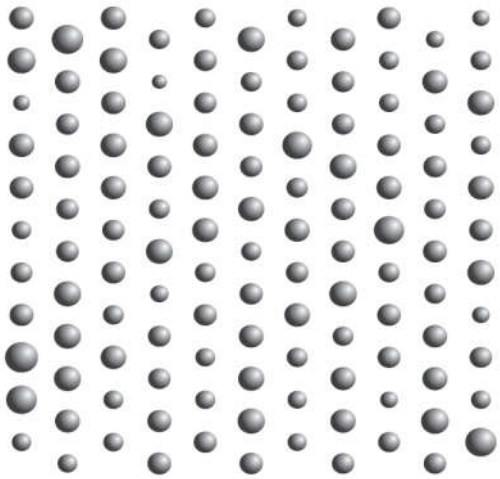

Figure 1. *Schematic diagram of 2D closed packed array of palladium nanoparticles.*

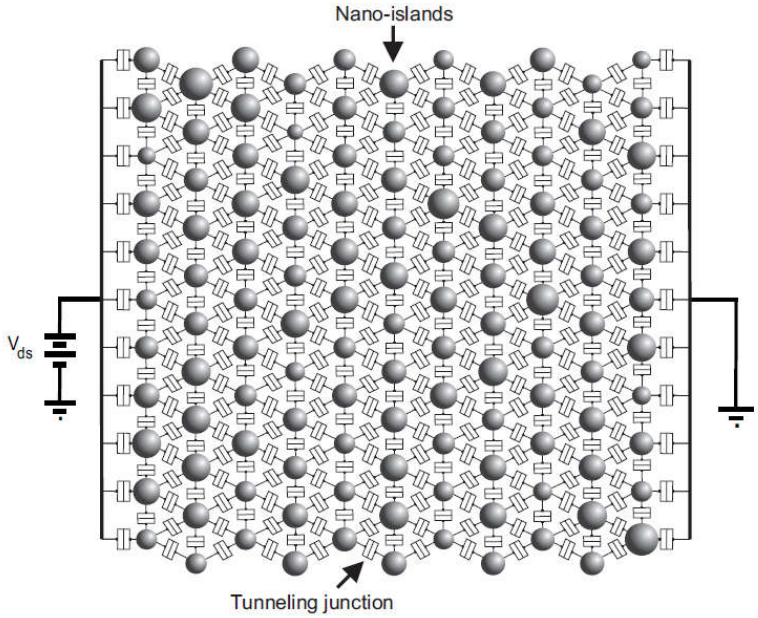

Figure 2. *Schematic circuit diagram of 2D hexagonal closed packed array of palladium nanoparticles.*

Orthodox theory is a semi-classical approach, which assumes that (i) the energy spectrum of the conductive islands may be considered continuous (ii) the tunneling time is negligible compared to the time between tunneling events, and (iii) coherent tunneling events are ignored [8].
The essential parameters in multi-island single-electron arrays are resistance and capacitance of tunneling junctions. We assume that the resistance of tunneling junctions can be described by [15]:

$$R \propto e^{\beta L} e^{E_C/kT} \quad (1)$$

Where L is the size of the tunneling gap. Here, the activation energy E_C is the Coulomb charging energy and β is a system dependent tunneling constant given by $\beta = \sqrt{8mU_0/\ ^2}$ [15], with m as effective mass of an electron. For avoiding several simultaneous tunneling, minimum tunnel resistance of all the tunnel barriers must be much higher than quantum unit of resistance

R_Q ($R \gg R_Q = \ /e^2 \sim 26.5\ K\Omega$),
where e is the elementary charge of electron and is Plank constant [16, 17].
We used an analytical method employing image charges for the calculation of junction capacitances C_{ij} between neighboring islands [18, 19]:

$C_{ij} = \frac{4\pi\epsilon_0 ab}{c} \sinh(U) \sum_{n=1}^{\infty} [\sinh(nU)]^{-1}$ (2)

Where a and b are the radii of palladium nanoparticles and dimensionless parameter U is related to a, b and c by $\cosh(U) = \frac{c^2 - a^2 - b^2}{2ab}$. Here, c is the center-center distance between adjacent palladium nanoparticles. We employed the extracted size distribution of nanodots in the tunneling resistance and capacitance calculations.
It is well known that palladium nanoparticles form hydride phases which absorb a substantial quantity of hydrogen within their crystal lattice. At room temperature, palladium hydrides may contain two crystalline phases, α and β (sometimes called $\acute{\alpha}$). Therefore, lattice parameter of palladium nanoparticles show hysteresis loop during adsorption and desorption of hydrogen. Bridget Ingham and coworkers have investigated the behavior of bare palladium upon hydrogen gas and they obtained variation of lattice parameter versus hydrogen pressure [13]. In the curves obtained by them both α and β phases are taken into account. We use the results obtained by them for lattice parameter of selected sizes of 3 and 6.1 nm in our studies. Expansion of individual nanoparticles increases the area occupied by each nanoparticle and this in turn decreases the average size of the tunneling gap. Thus, according to the equations (1) and (2), the resistance and capacitance of tunneling junctions change.
Owing to the expansion of palladium nano-islands, we employ following steps in order to calculate new resistance and capacitance of the tunneling junctions. (1) A change (a) occurs in the lattice parameter (a) due to the change in the external hydrogen pressure. (2) The variation (a) in lattice parameter causes the change (d) in diameter (d) of palladium nanoparticles ($d = (\ a/a)d$). (3) Expansion of individual nanoparticles increases the area occupied by each nanoparticle and this in turn decreases the average size of the tunneling gap (L). In general, the change in L is given by

$$L = \ (pd/\ L)\ \alpha. \quad (4)$$

Therefore, according to relations (1) and (2), the resistance and capacitance of tunneling junctions change. Furthermore, the temperature of 300 K (the temperature for detecting hydrogen) was used in simulations. In reality, hydrogen will change slightly the band in palladium nanoparticles, and accordingly will change β in expression (1) as well. We found this effect not important in the IV characteristics and in the following the change in tunneling gap (L) was only considered. After setting some parameters like temperature, mode of simulation, resistance and capacitance of tunneling junctions, we inspected IV characteristics.

3. RESULTS AND DISCUSSION

Fig. 3 shows the I_{ds}-V_{ds} at room temperature.

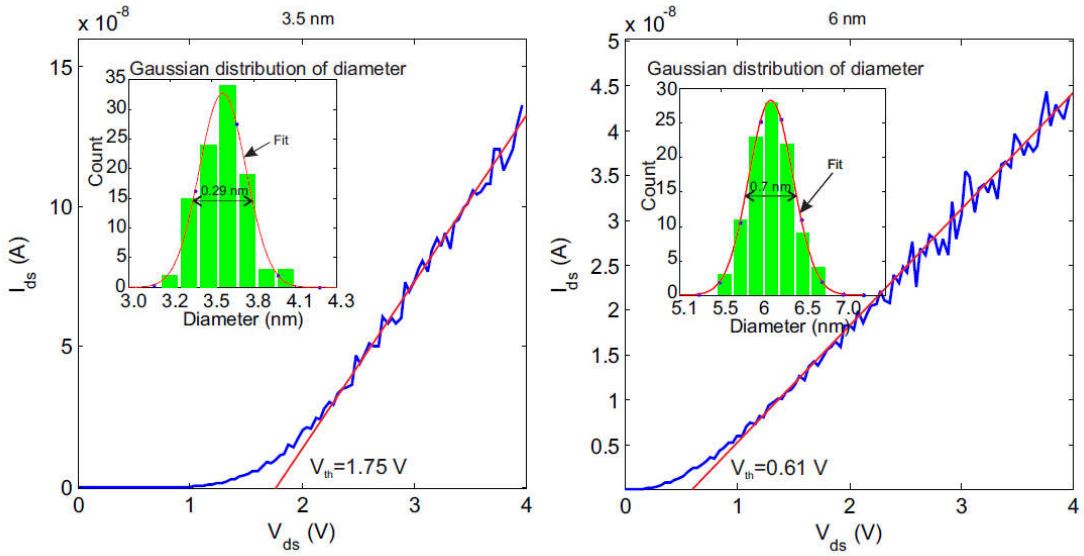

Figure 3. *I_{ds}-V_{ds} characteristics of arrays, respectively, for 3, and 6 nm nano-islands simulated at T = 300 K.*

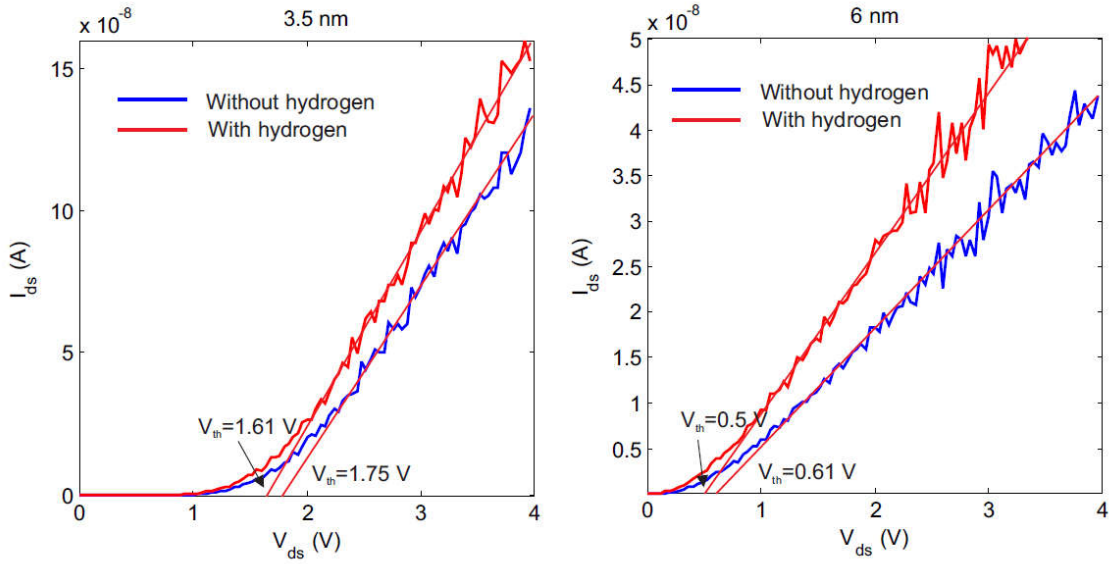

Figure 4. *I_{ds} -V_{ds} characteristics of arrays, respectively, for 3, and 6 nm nano-islands before and after exposure to hydrogen simulated at T = 300 K.*

Also, the size distribution of nanoparticles obtained from TEM image of synthesized arrays is shown in this figure. Coulomb blockade are clearly observed. At bias voltages more than threshold voltage the dc curve gradually approaches to offset linear asymptotes. Extrapolation of the linear regions results in a V_{th} of 1.75 and 0.61 V, respectively, for arrays with mean diameter of 3.5 and 6 nm which represent the basic conceptual principle of threshold voltage [20]. We remark that the current suppression region for arrays with mean diameter of 3.5 nm is greater than the ones with mean diameter of 6 nm. In the literature, Coulomb blockade threshold for a 1D array of nano-islands is inversely related to the capacitance; therefore, the

decrease in current suppression region (Coulomb blockade) is probably due to the increase in the total capacitance of the array.

The possibilities of using these arrays as single-electron tunneling based hydrogen sensor were put into investigation. IV characteristics of the arrays were inspected upon exposure to hydrogen gas. We selected hydrogen pressure of 20 torr for our investigation. The lattice parameters of 3 and 6.1 nm palladium nanoparticles were extracted for 20 torr, which are provided in Table 1. The change in tunneling resistance and capacitance was calculated for each tunneling junction according to the procedure mentioned in the assumptions of the model. Then IV characteristics with new parameters were plotted. Fig. 4 shows the IV characteristics of the arrays before and after exposure to hydrogen. As can be seen in Fig. 4, by exposing the arrays into hydrogen gas, IV characteristics separate before and after the exposure to hydrogen. The reason for increasing electrical current is as follows; expansion of individual nanoparticles increases the area occupied by each nanoparticle and this in turn decreases the total resistance of the arrays (due to decrease in the tunneling resistance of adjacent nanodots).

Also shown in Fig. 4 are the linear extrapolations to zero electrical current. For IV characteristics of 3.5 and 6 nm arrays obtained upon hydrogen gas, extrapolation of the linear region results in a V_{th} of 1.61 and 0.5 V, respectively. We remark that, the decrease in the coulomb blockade threshold here is related to the increase in the total capacitance of the arrays.

An important factor in hydrogen sensors is their response. Typically metal hydrogen sensors measure resistance changes under a fixed applied voltage [3]. Detection is based on a change in electrical resistivity following absorption of hydrogen from the ambient due to the higher electrical resistance of palladium hydride compared with palladium. In our proposed sensor, the resistance at voltages greater than current restriction region can be used in order to detect hydrogen gas. For example, at selected partial pressure of 20 torr for hydrogen gas our proposed sensor can detect 1.3% hydrogen gas in air which is less than flammability concentration of hydrogen gas. Though, selected pressure of 20 torr was used in the simulations. It is possible to use lower pressures which means even lower pressures can be detected. On the other hand, since this sensor is based on the single-electron tunneling between palladium nano-islands, this sensor is an ultra-low power consumption sensor.

4. CONCLUSION

In this paper we demonstrated single electron tunneling effect and emergence of Coulomb blockade in the 2D hexagonal closed packed array of palladium nanoparticles. Also, we inspected possibilities of using these arrays as single-electron based hydrogen sensor. First, arrays of monodisperse palladium nanoparticles with Gaussian distribution in size were assumed between two electrodes. Then, I_{ds}-V_{ds} characteristics were obtained from equivalent circuits. Coulomb blockade were clearly observed. According to the linear extrapolations to zero, current suppression region increased with decreasing mean size of the arrays. Also, upon hydrogen gas, coulomb blockade region decreased for arrays which may be due to the change in total capacitance of the array. A hydrogen sensor was successfully designed from these arrays which could detect concentrations lower than flammability limit.

REFERENCES

1. Jacobson, M. Z., Colella, W. G., Golden, D. M. (2005) . “Cleaning the air and improving health with hydrogen fuel-cell vehicles”, *Science*, 308: (5730) 1901-1905.

2. Liekhus, K. J., Zlochower, I. A., Cashdollar, K. L., Djordjevic, S. M., Loehr, C. A. (2000). "Flammability of gas mixtures containing volatile organic compounds and hydrogen", *Journal of Loss Prevention in the Process Industries,* 13: (35) 377- 384.
3. Hbert, T., Boon-Brett, L., Black, G., Banach, U. (2011). "Hydrogen sensors a review", *Sensors and Actuators B: Chemical*, 157: (2) 329-352.
4. Xie, B., Liu, L., Zhang, Y., Peng, X., Xu, Q., Zheng, M., Song, F., Wang, G., Han, M., Takiya, T., "Dense palladium nanoparticle arrays with controlled coverage for fast hydrogen sensors", in: Nano/Micro Engineered and Molecular Systems (NEMS), 2011 IEEE International Conference on, IEEE, 2011, pp. 25-28.
5. Zhang, P., Deshpande, S., Seal, S., Cho, H., Medelius, P., "Fast detection of hydrogen at room temperature using a nanoparticle-integrated microsensor", in: Sensors, 2006. 5th IEEE Conference on, 2006, pp. 712-715.
6. Kim, S.-W., Park, J., Jang, Y., Chung, Y., Hwang, S., Hyeon, T., Kim, Y. W. (2003). "Synthesis of monodisperse palladium nanoparticles", *Nano Letters*, 3: (9) 1289-1291.
7. Park, J., An, K., Hwang, Y., Park, J.-G., Noh, H.-J., Kim, J.-Y., Park, J.-H., Hwang, N.-M., Hyeon, T. (2004). "Ultra-large-scale syntheses of monodisperse nanocrystals", *Nature materials*, 3: (12) 891-895.
8. Likharev, K. (1999). "Single-electron devices and their applications", *Proceedings of the IEEE*, 87: (4) 606-632.
9. Zhang, X., Chi, Y., Fang, J., Zhong, H., Chang, S., Fang, L., Qin, S., (2010). "Single electron transistor with programmable tunnelling structure", *Physics Letters A*, 374: (48) 4880-4884.
10. H. Mehrara, A. Erfanian, M. Khaje, M. Zahedinejad, F. Rezvani, Iv characteristics of two-dimensional nanodot-array single electron transistors, Superlattices and Microstructures 53 (0) (2013) 1-8.
11. Karre, P., Acharya, M., Knudsen, W., Bergstrom, P. (2008). "Single electron transistor-based gas sensing with tungsten nanoparticles at room temperature", *Sensors Journal, IEEE*, 8: (6) 797-802.
12. Fujino, H., Oya, T. (2014). "Analysis of electron transfer among quantum dots in two-dimensional quantum dot network", *Japanese Journal of Applied Physics*, 53: (6S) 06JE02.
13. Ingham, B., Toney, M. F., Hendy, S. C., Cox, T., Fong, D. D., Eastman, J. A., Fuoss, P. H., Stevens, K. J., Lassesson, A., Brown, S. A., Ryan, M. P. (2008). "Particle size effect of hydrogen-induced lattice expansion of palladium nanoclusters", *Phys. Rev.*, B 78: 245408.
14. Wasshuber, C., Kosina, H. (1997). "A single-electron device and circuit simulator", *Superlattices and Microstructures*, 21: (1) 37- 42.
15. Barwiski, B. (1987). "Temperature dependence of the electrical conduction in discontinuos silver films on sapphire substrates", *Thin Solid Films*, 148: (3) 233-241.
16. Averin, D., Odintsov, A. (1989). "Macroscopic quantum tunneling of the electric charge in small tunnel junctions", *Physics Letters A*, 140: (5) 251-257.
17. Geerligs, L. J., Averin, D. V., Mooij, J. E. (1990). "Observation of macroscopic quantum tunneling through the coulomb energy barrier", *Phys. Rev. Lett.*, 65: 3037-3040.
18. Pisler, E., Adhikari, T. (1970). "Numerical calculation of mutual capacitance between two equal metal spheres", *Physica Scripta*, 2: (3) 81.
19. Lekner, J. (2011). "Capacitance coeffcients of two spheres", *Journal of Electrostatics*, 69: (1) 11-14.
20. Ortiz-Conde, A., Snchez, F. G., Liou, J., Cerdeira, A., Estrada, M., Yue, Y. (2002). "A review of recent MOSFET threshold voltage extraction methods", *Microelectronics Reliability*, 42: (45) 583-596.